Available online at www.sciencedirect.com
SCIENCE DIRECT
ELSEVIER
Journal of the European Ceramic Society 26 (2006) 1003–1011
ECERS
www.elsevier.com/locate/jeurceramsoc

# Contact residual stress relaxation in soda-lime glass Part I. Measurement using nanoindentation

Kwadwo Kese *, Matilda Tehler, Bill Bergman

*Department of Materials Science and Engineering, Royal Institute of Technology, 10044 Stockholm, Sweden*

Received 28 August 2004; received in revised form 3 December 2004; accepted 10 December 2004
Available online 26 February 2005

**Abstract**

The contact residual stress field created by a Vickers indentation is a micro-size region of high and varying stresses. Stress relaxation studies in such a micro-region may not be accessible to the conventional methods of investigation. In this paper the elastic response during nanoindentation has been used to study the isothermal stress relaxation of a Vickers residual stress field in soda-lime glass at 540 and 630 °C. At each temperature, the stress relaxation profile varied from one location of the stress field to the other suggesting non-linear response to stress. Also, the relaxation profiles at identical positions were different for the two temperatures suggesting that the Vickers residual stress field is not a thermorheologically simple region of material.


*Keywords:* Nanoindentation; Glass; Stress relaxation

## 1. Introduction

When a Vickers indentation is made in soda-lime glass, residual stresses are created, because a plastically deformed region is formed beneath the surface impression. Around this plastic region, the material is permanently strained elastically, thus leaving the surrounding matrix in a state of stress. During subsequent testing of a specimen containing a Vickers flaw to measure the fracture strength, $\sigma_f$, or the fracture toughness, $K_{IC}$, the residual stresses act together with the applied stress, $\sigma_a$, in determining the fracture mechanics of the material as expressed by the following relationship:

$$K = \chi_r \frac{F}{c^{3/2}} + \phi\sigma_a\sqrt{c}, \quad (1)$$

where $K$ is the stress intensity factor; $F$, the maximum load in making the Vickers indent; $\sigma_a$, the stress applied during the fracture testing; $\phi$, a crack geometry factor; $\chi_r$, a characteristic of the residual stress field.

The residual stresses, represented by the first term on the right hand side of Eq. (1), have been determined[1,2] to impact on both the static and dynamic fatigue properties of brittle solids. Inclusion of the residual contact term in the analysis, however, is not straightforward: as the residual field strength changes due to ageing, so is $\chi_r$ expected to change. The value of $\chi_r$ used in a particular analysis must, therefore, reflect these varying conditions. A way to avoid the uncertainties that inaccurate determination or choice of $\chi_r$ might entail has been to remove the residual contact stresses either by annealing or polishing away the plastic zone surrounding the indentation.[3] Salomonson and Rowcliffe[4] employed both methods and found polishing to be the more effective method of the two. In the case of annealing, they observed full relief of the original tensile stresses after holding at 550 °C for 24 h. Studies by Marshall and Lawn,[1] Chantikul et al.,[2] and Roach and Cooper[5] have also shown how annealing can reduce or remove the residual stresses around an indentation thereby enhancing the fracture properties.

This paper is about the kinetics and extent of stress relief achieved around the Vickers indent during isothermal annealing of a sample containing the Vickers defect. The method of investigation derives from an observed[6] dependence of the

* Corresponding author. Tel.: +46 8 7909134; fax: +46 8 207681.
*E-mail address:* kese@mse.kth.se (K. Kese).

0955-2219/$ – see front matter © 2005 Elsevier Ltd. All rights reserved.
doi:10.1016/j.jeurceramsoc.2004.12.029

nanoindentation elastic modulus on the applied (or residual) stress state in a soda-lime glass. The Vickers residual stress field is a micro-size region of high and varying stresses. Stress relaxation studies in such a small region may not be accessible to the conventional methods of stress measurement. For example Roach and Cooper,[5] Arora et al.,[7] and Han et al.[8] performed optical retardation measurements at the edge of the Vickers indent and used it as a measure of the extent of residual stress decay in the entire stress field. Although very useful results were obtained, such a method does not permit a detailed profiling of the stress field as a function of annealing temperature and time. On the other hand, the high spatial resolution capacity ($\sim \pm 400$ nm) of nanoindentation permits almost a point-to-point measurement of the entire stress field after any prescribed annealing treatment.

In sub-micron depth-sensing indentation experiments (also known as nanoindentation) the load $P$, and the depth of penetration $h$, are continuously recorded throughout the indentation cycle. The depth $h$, together with the known geometrical shape of the indenter is then used in the subsequent determination of the area of the residual impression generated. Oliver and Pharr[9] developed a method for determining the hardness and elastic modulus from data obtained from depth-sensing indentation experiments. For the Berkovich tip, the contact area of the indentation is obtained as:

$$A = 24.56h_c^2, \tag{2}$$

where $h_c$ is the depth along which the indenter and the sample are in contact at maximum load.

The effective modulus $E^*$, of the elastic–plastic contact between the specimen and the indenter then incorporates the area $A$ as:

$$E^* = \frac{1}{\beta}\frac{\sqrt{\pi}}{2}\frac{S}{\sqrt{A}}, \tag{3}$$

where $S$ (=d$P$/d$h$) is the contact stiffness calculated at maximum load $P_{max}$, and $\beta$ is an indenter geometry constant. If $E_i$ denotes the elastic modulus of the indenter, then that of the sample, $E$, may be obtained from the expression

$$E = \frac{1-\nu^2}{1/E^* - (1-\nu_i^2)/E_i}, \tag{4}$$

where $\nu_i$ and $\nu$ represent the Poisson ratios of the indenter and sample, respectively. The sample hardness, $H$, is also calculated using the contact area and the maximum load, $P_{max}$, as

$$H = \frac{P_{max}}{A}. \tag{5}$$

In a study to investigate the influence of applied or residual stress on the elastic modulus and hardness, Kese et al.[6] found that the elastic modulus of soda-lime glass measured by nanoindentation was influenced by the presence of the stresses in the sample. The present paper attempts to utilise the observed dependence of nanoindentation elastic modulus, $E$, on stress, in the study of stress relaxation in soda-lime glass. That the elastic modulus of soda-lime glass can change due to the presence of applied stresses was established long ago by Mallinder and Proctor.[10,11]

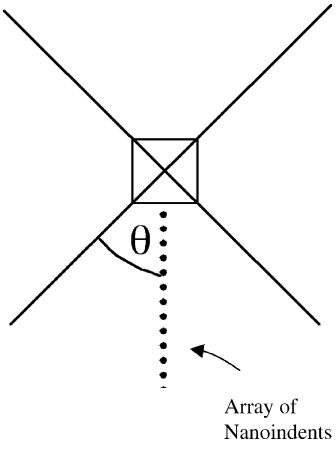


Fig. 1. Showing the loci of indents as used in this study ($\theta = 45^\circ$).

In the present study, first, $E$ was measured in a stress-free specimen and was found to be constant with a maximum scatter around the mean, $E_{av}$, of $\pm 0.5$ GPa. The experiment was then repeated, but this time close to a Vickers impression where residual stresses are known to exist, Fig. 1. Close to the indent, a systematic change of $E$ with position was observed, Fig. 2. At far away distances from the impression, where the influence of the residual stress field is low or approaching zero, $E$ became constant with the same scatter as mentioned above. In a stress-free soda-lime glass specimen or one with a constant surface-stress, the characteristic data scatter about the mean, was therefore, less than $\pm 0.5$ GPa in the present study. The difference between the elastic modulus measured close to the edge of the Vickers impression and the mean, $E_{av}$, was greater than 16 GPa. Far exceeding the characteristic data scatter of the method this meant that the elastic response to stress around the Vickers indent is a real and experimentally measurable effect.

These preliminary experiments thus assured the reliability of the nanoindentation elastic response as a tool for

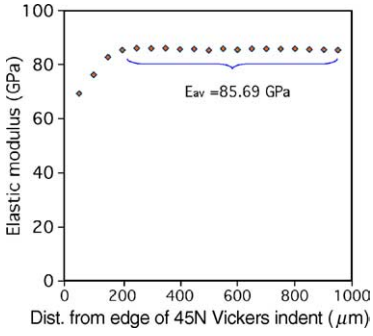


Fig. 2. Elastic modulus, $E$, as a function of position in the residual stress field of a 45 N Vickers indent in soda-lime glass. $E$ shows a systematic variation with distance with approach towards the edge of the indent, while it is not affected at far away distances from the edge of the indent.

investigating the stress field around the Vickers indent in glass. The potential of the nanoindentation elastic response as a stress probe has already been observed and reported by other workers.[12–14] Apart from the elastic response, there are other features associated with indentation in materials that can also serve as stress tell-tales. For example, the shape of the pileup that surrounds an indentation can be used to determine the level of residual stresses present:[15] thus using an optical interference method Underwood[16] was able to measure the magnitude and sign of residual stress in steel by studying the deviations in shape of the pileup surrounding spherical indentations in samples of the material. The residual stress field around the Vickers indent being non-equal biaxial,[17–19] the elastic response measured here may be regarded as relating to an average stress at each location of nanoindentation.

## 2. Method

The specimens used in this study were 3-mm-thick float glass plates (nominally 12.5 mm × 12.5 mm) preannealed at 630 °C for 1 h to remove any existing fabrication surface stresses. The experimental procedure consisted of three main parts: (i) generation of residual stress in the specimens, (ii) taking the samples through annealing schedules with the aim of relieving the stresses generated in (i), and (iii) performing nanoindentation tests in order to follow the process of stress relaxation attending to part (ii). Generation of residual stress in the specimens was achieved by introducing a Vickers indentation into one face of each specimen using a load of 45 N. The residual stress thus generated was biaxial around the Vickers impression.[17] One of the samples, which was not to be subjected to any further annealing beyond the preannealing exercise was glued to an aluminium block and mounted on the nanoindenter (NANO INDENTER®II, Nano Instruments, Inc., Oak Ridge, TN) and allowed to thermally equilibrate for several hours. A nanoindentation experiment was run along a chosen radial direction $\theta$ (=45°) with respect to a radial crack as illustrated in Fig. 1. The rest of the samples, each also containing a Vickers indent were annealed for various hold times: 0, 4 and 24 h at 540 °C and 0, 0.25, 0.5, 1.75 and 2 h at 630 °C. The choice of these temperatures was to study the role of conditions below and above $T_g$ (=566.5 ± 2.5 °C as measured by the DSC method) on the kinetics of stress relaxation around the Vickers defect in glass. The heating rate was ∼21 °C/min while the cooling rate was ∼1.5 °C/min. After annealing, a nanoindentation experiment was performed on each of the specimens in the same manner as described above, Fig. 1. Each nanoindent was made using one cycle of loading and unloading, with two constant-load hold segments inserted at peak load and 90% unload. The peak load was 25 mN. The first constant-load hold segment was to measure and account for creep at maximum load while the second was to measure and account for the thermal drift coming from the instrumentation.

## 3. Results and discussion

### 3.1. Effect of annealing on elastic modulus measured in the Vickers residual stress field

In the Vickers contact residual stress field, the stresses are high near the edge of the impression and decrease with distance away from it. As mentioned in the introduction the nanoindentation elastic modulus seems to reveal the presence of stress in a material, a fact that is clearly demonstrated by the example of Fig. 2, where $E$ decreases continuously with approach towards edge of the Vickers indent.

The sample of Fig. 2 was nanoindented directly after introducing the Vickers indent in the preannealed sample, without any intervening annealing. Further annealing (temperature and hold time as variable parameters) of the Vickers contact residual stress field caused $E$ to increase toward the equilibrium stress-free value of the glass. As the effect of further annealing is to relieve stresses among other things, this response of the elastic modulus to annealing can be related to the stress relaxation around the Vickers indent. That is, stresses cause $E$ to decrease relative to the stress-free value of the material; as annealing relieves the material of the stresses, $E$ tends to revert back to the stress-free value.

A problem with experiments using the Vickers residual stress quadrant is that in practice no two quadrants are identical. Therefore, nanoindentation measurement of properties at identical positions of different stress quadrants may not always yield exactly the same results. For example tests done on several ‘no anneal’ samples gave results that formed a band of $E$ values, Fig. 3, instead of coinciding into a single-line plot. This spread in results is not due to the nanoindentation method. Rather it is due to the physical condition of each Vickers indentation and its residual stress quadrants, coming possibly from differences in: (i) radial/lateral crack sizes and the residual stress relaxation resulting from the slow crack growth of these cracks, (ii) processes occurring at the edge

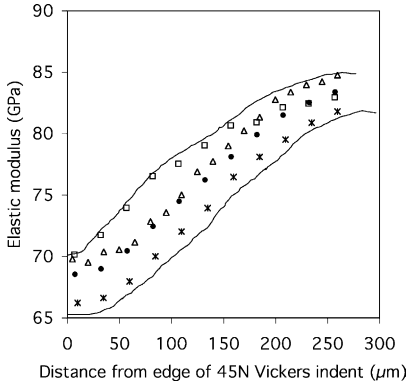


Fig. 3. Physical differences between different stress quadrants may lead to variation in property values measured at identical points in the stress fields. Here the elastic modulus measured along identical loci in the residual stress quadrant of different ‘no anneal’ samples fall within a band of values instead of forming a single line plot as one would expect in an ideal case.

of an indent such as piling-up, and (iii) sample surface and mounting conditions.

This, therefore, leads to an uncertainty when data must be collated, as in this study, from measurements done in different stress quadrants in order to study an effect. In general one would expect the $E$-plots for different hold times to be vertically displaced relative to one another, i.e., longer hold times should shift the $E$-plot towards the equilibrium stress-free value. In practice, however, results from some of the different hold times overlapped: i.e., some of the $E$-plots crossed each other. For the 630 °C tests the following assumption was made in collating the elastic modulus data for the present study. For hold times $t_1$ and $t_2$ ($t_2 > t_1$), the $E$-plot of $t_2$ should lie above that of $t_1$ in general agreement with the fact that longer hold times should lead to more stress relaxation, and a relative upward shift of the $E$-plot toward the stress-free value. The same assumption was made for the 540 °C tests except that in this case cross-over of data plot was allowed for the 24 h results since repetition of that test consistently showed a tendency for part of the $E$-plot to lie at a position below the expected. As will be explained in Section 3.5, this behaviour at temperatures below $T_g$ happens to be a subtle but real effect which, although easily and consistently registered by the nanoindentation method, would go undetected if one were only to measure a representative stress decay at the edge of the impression as in the optical retardation method.

### 3.2. Relating the elastic response to stress

The general effect of annealing a mechanically strained region of soda-lime glass is thus to increase the nanoindentation elastic modulus, $E$, towards the stress-free value of the glass. For example, annealing for 2 h at 630 °C increases the elastic modulus at a distance of less than 10 μm from the edge by about 16 GPa while the corresponding increase at far away distances is about 2 GPa. As pointed out above such an $E$-plot could also be related to the extent of stress relaxation achieved at those locations due to annealing. The result of Mallinder and Proctor[10,11] is used here as a first approximation to convert the elastic modulus to stress. For soda-lime glass they found the elastic modulus, $E$, to depend on the strain, $\varepsilon$, as:

$$E = E_o - 5.11E_o\varepsilon, \tag{6a}$$

from which the strain can be solved as

$$\varepsilon = \frac{E_o - E}{5.11E_o}. \tag{6b}$$

For a material which shows non-linear elastic behaviour, within a small strain interval, d$\varepsilon$, a constant elastic modulus may be assumed to relate the stress, $\sigma$, to the strain as:

$$\frac{d\sigma}{d\varepsilon} = E, \tag{7}$$

which gives

$$\int d\sigma = \int E d\varepsilon \tag{8a}$$

$$\sigma = \int (E_o - 5.11E_o\varepsilon)d\varepsilon + C \tag{8b}$$

after substitution from (6a).

At $\varepsilon = 0$, $\sigma = 0$ gives $C = 0$ in (8b).

The stress is thus obtained as

$$\sigma = E_o(\varepsilon - 2.55\varepsilon^2). \tag{9}$$

Substituting $\varepsilon$ from (6b) into (9) gives a relation between the stress and the elastic modulus:

$$\sigma \approx \frac{1}{10.22E_o}(E_o^2 - E^2). \tag{10}$$

Fig. 4 show stress relaxation diagrams obtained after applying Eq. (10) to $E$-data measured in the Vickers residual stress field. A fourth power polyfit curve is applied to each set of data to obtain a continuous stress function for each hold time across the stress field. The distance, $x$, from the edge of the indent is normalised with the size, $d$, of the indent (=half the length of diagonal of the plastic impression = 61.5 μm). It must be pointed out that the stresses calculated in this study

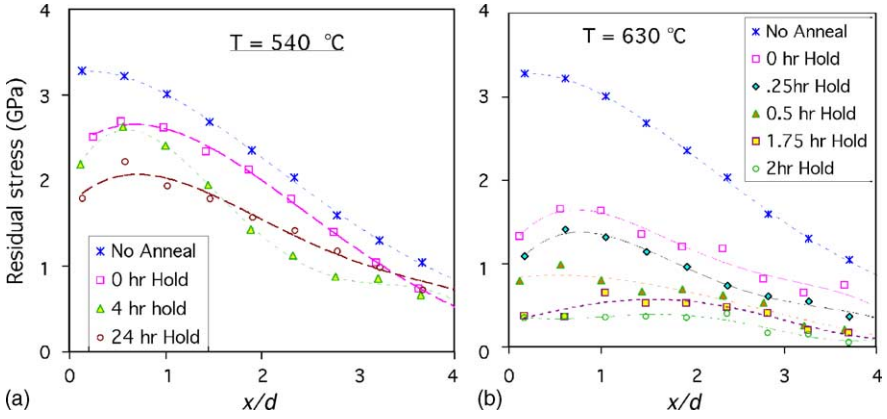


Fig. 4. Residual stress relaxation around a Vickers indent as function of annealing hold time: (a) results after annealing at 540 °C and (b) results after annealing at 630 °C.

using Eq. (10) may only be approximate since Mallinder and Proctor[10] considered only uniaxial stresses in their study. However, since normalised quantities are used in relaxation studies, any discrepancies in absolute values will not detract from the qualitative discussion. In addition, the 'no-anneal' curves of Fig. 4 have a similar form to what has been obtained from experimental stress measurement in the Vickers residual stress field.[17,19] Close to the edge of a sharp indent in soda-lime glass the theoretical result of Chiang et al.[20] predicts a residual tensile stress ($\sigma_{yy}$) of ~0.98 GPa (when $H = 5.5$ GPa) and appreciably high compressive stresses ($\sigma_c$). The ratio, $\sigma_c/\sigma_{yy}$, of the compressive-to-tensile stresses close to a Vickers indentation in soda-lime glass has been determined in micro-indentation fracture measurements[17,18] to be ~4 and in a nanoindentation fracture measurement[19] to be ~6. The stresses measured here for the 'no-anneal' indents shown in Fig. 4 are, therefore, reasonable approximation average values. Eq. (10) means that as the stress tends to low values, $E$ approaches $E_o$. $E_o$ can be the elastic modulus of a stress-free specimen.

In Section 3.1 we discussed the problem associated with measuring mechanical properties using different quadrants of the Vickers indent. Fig. 5 is an example of stress plots obtained from measurements done in one and the same stress quadrant of a Vickers indentation. An array of nanoindents was first made in one of the four quadrants formed by the radial cracks of a non-annealed Vickers indentation; the sample was then annealed for 1 h at 630 °C after which a second nanoindentation measurement was done in-between the nanoindents of the first array. ADEF is the result after annealing for 1 h at 630 °C while CDEF is the results of the as-indented experiment. BD is an imaginary stress decay path that would be expected from an extension from point D. Why ADEF is the relaxation path, instead of BDEF will be explained below. As may be seen in the figure, the region beyond $x = 3d$ shows unchanging elastic modulus after heating to and holding for 1 h at 630 °C. Beyond $x = 6d$ (point E)

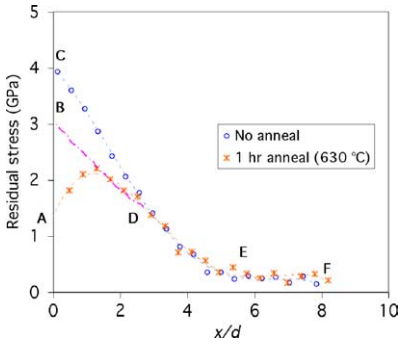


Fig. 5. Residual stress plot for two experiments performed consecutively along the same direction in the same Vickers residual stress field. The first experiment was performed when the sample containing the Vickers system was not annealed (plot CDEF). After this, the sample was annealed 1 h at 630 °C after which the second experiment was performed with the new set of nanoindents carefully placed in between the indents of the first experiment (plot ADEF). BD is an imaginary relaxation segment.

the elastic modulus is constant with respect to both position and thermal history. With prolonged hold at the annealing temperature, AD will flatten out as D shifts towards the right until it coincides with the constant modulus segment (EF) at complete residual stress relaxation. This is what would happen if transient relaxation of one and the same residual stress quadrant were continuously studied during the annealing exercise. Due to path hysteresis during thermal cycling of glass, it was deemed inadvisable, in the present study, to re-anneal a particular stress quadrant beyond the first annealing. Shen et al.[21] found that thermal history could influence the stress relaxation behaviour of glass.

Figs. 4 and 5 clearly reveal a peculiarity associated with stress relief close to a defect: that of a region of fast relieving stresses, adjacent to the edge of the defect, leading to an initial dip in the stress relief curve. Such a behaviour was also found by Salomonson and Rowcliffe[4] and James,[22] the latter, during a study of fatigue stress relaxation in an aluminium alloy where the stress relaxation was found to be faster close to the surface. Also, in glass seals, the seal edges have been observed to relax more than the bulk material.[23] The reason behind this behaviour in the Vickers residual stress field will be explained in the next sub-section.

### 3.3. Influence of annealing on the plastic zone

It is instructive to consider the behaviour of the plastic zone during annealing since it is the raison d'être of the residual stress field around the Vickers indent. Getting rid of the plastic zone should remove the strains imposed on the surrounding matrix and result thus in stress relief. Also, since the formation of a plastic zone in soda-lime glass involves elastic deformation, densification and plastic deformation, removing the plastic zone should logically involve a reversal of these forms of material deformation. Of the three, elastic deformation is the one that recovers first, occurring already in connection with load withdrawal. The other two can only be reversed through heating near $T_g$.[4,24] In another study, by Kese and Tehler,[25] the response of the plastic zone to annealing was investigated by examining the fracture surfaces of samples annealed at different temperatures and hold times. Fig. 6 shows a sketch of the main points of the results that were obtained. Fig. 6(a) is an illustration of the plastic deformation zone before annealing, showing the shear deformation flow lines (see Hagan[26]), while Fig. 6(b) and (c) illustrate the plastic deformation zone at various stages of annealing. The grey areas represent plastically deformed material, while the white areas below the Vickers impression represent plastic areas that have been transformed.

As illustrated in Fig. 6, the study showed that the plastically deformed region responds to annealing by first 'dissolving' itself in its interface region with the Vickers indent. In other words, reverse transformation of the plastic zone starts from the Vickers indent and proceeds radially outwards towards its boundary with the material matrix. The effect of

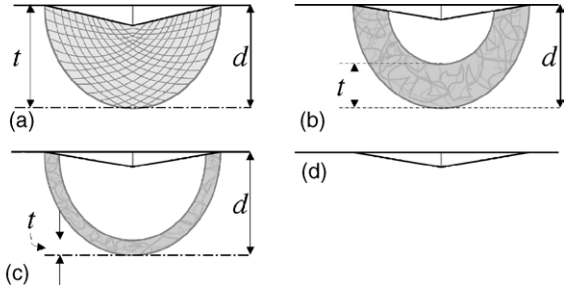


Fig. 6. Schematic diagram showing the transformation of the plastic zone beneath the Vickers indent during annealing. (a) The plastic zone is in the form of a solid hemisphere with a characteristic size, $d$. (b) The transformation of the plastic zone begins at its interface region with the indent. As annealing progresses, the solid hemisphere is transformed into a shell of plastically deformed material containing a mass of transformed material within its cavity; the thickness of this shell is $t$ but the outer dimension of the plastic zone remains unchanged. (c) Extended annealing, especially at temperatures above $T_g$ results in further thinning out of the shell of the plastic zone; $t$ thus decreases while $d$ remains unchanged. (d) With prolonged annealing at temperatures above $T_g$, the plastic zone is completely transformed and there is no plastically deformed material surrounding the indent. There is thus a preferred direction in which the transformation of the plastically deformed region occurs.[25]

this preferred direction of plastic zone annihilation is that the initial solid volume is changed to become a shell of plastically deformed material holding within its cavity, a mass of reverse-deformed material. The size (or outer dimension) of this shell remains virtually constant throughout the annealing process but its thickness decreases constantly. The kinetics and nature of stress relaxation that takes place in the Vickers residual stress field should be linked with what happens at and inside this shell. The 'dip' (or the fast relieving stresses) in the relaxation curves close to the edge of the Vickers indent (for example, path ADEF of Fig. 5) can thus be explained to be due to the quick reverse transformation back to undeformed material that occurs in the interface region adjacent to it. The mechanism here could be that of volume restoration, which is favoured by proximity to the region of fast transforming material. With increasing distance from the edge, the effect of the transformed region on relaxation decreases, less stress is thus relaxed, and the stress relaxation curve rises. Segment DA of Fig. 5 corresponds to this type of relaxation. In the absence of the effect of the transformed plastic region, the path of relaxation would follow a curve like DB. The influence of the presence of the transformed plastic zone reaches a minimum, after which point other relaxation mechanisms begin to dominate at distances far from the indent. Fig. 7 shows some SEM pictures of the results of the reverse transformation process for different annealing temperatures and times.

### 3.4. Relaxation mechanisms in a mechanically deformed region

Comparing Fig. 4(a) and (b) it can be seen that the 630 °C curves are more flattened, whilst the 540 °C curves are steeper. Two main mechanisms may be considered to operate during annealing of a mechanically deformed region in glass: mechanical and chemical mechanisms. The mechanical processes, which may involve expansion and restoring bonds

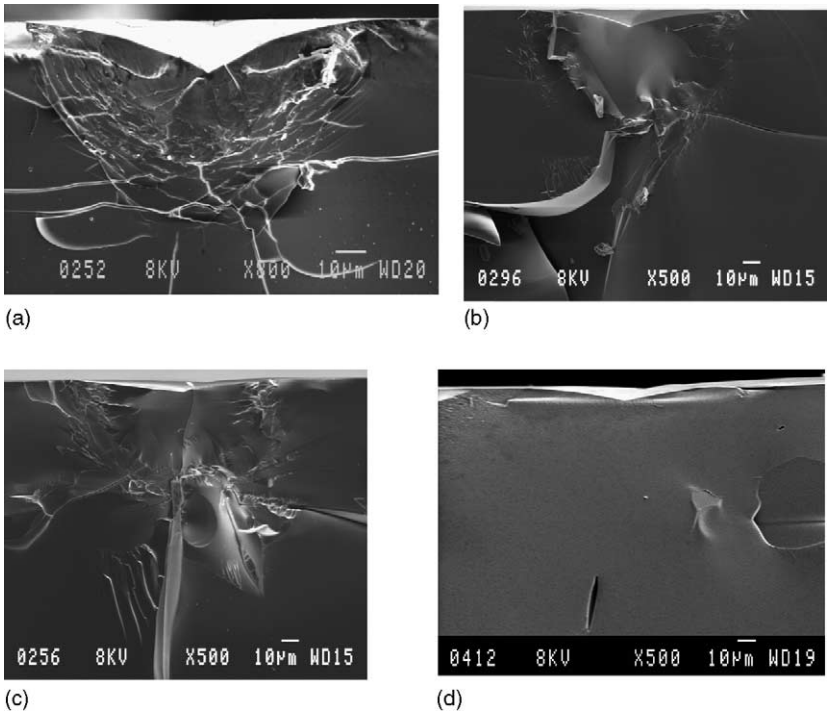


Fig. 7. SEM pictures of the plastic zone transformation process for selected temperatures and times as a further illustration of Fig. 8: (a) as-indented, no annealing, (b) annealed 24 h at 550 °C, (c) heated to 600 °C with 0 dwell time, and (d) annealed 24 h at 600 °C.[25]

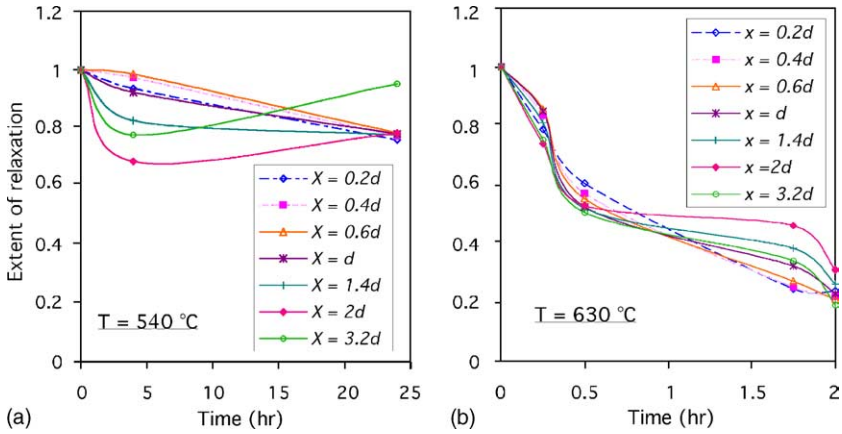


Fig. 8. Showing the influence of temperature on the kinetics of residual stress relaxation in the near-field of a Vickers indentation: (a) relaxation profiles after annealing at 540 °C and (b) relaxation profiles after annealing at 630 °C. The stresses are almost relaxed everywhere in the stress field at 630 °C while substantial amounts of stresses still remain in the stress field even after 24 h annealing at 540 °C. The curves joining the data points serve only to aid in perceiving general trends in relaxation at the two temperatures.

to their original mechanical equilibrium, have low activation energies and operate already at low temperatures. Operative at temperatures close to and above $T_g$, the chemical processes on the other hand, are characterised by high activation energies and are responsible for restoring the system to structural equilibrium. The mechanical processes, are therefore, the underlying relaxation processes unto which the chemical processes superimpose according as increasing temperatures make the latter more favourable. The difference in form noted above between the 540 and the 630 °C curves stems, therefore, from the heightened kinetics of the mechanical processes at 630 °C relative to that at 540 °C, in addition to the chemical processes now operative at the higher temperature. Bartenev and Scheglova[27] identify slow and fast processes, $R_1$ ($E_A$: ∼21 kJ/mol) and $R_2$ ($E_A$: ∼55 kJ/mol) respectively, predominant at low temperatures, and a chemical process $R_3$ ($E_A$: ∼251 kJ/mol), operative at temperatures close to and above $T_g$. $E_A$ represents the activation energy for each mechanism.

### 3.5. Graphical study of relaxation kinetics of the near-field region

As may be seen in Fig. 5, the region beyond D (∼$x = 3.2d$) from the edge virtually involves unchanging or constant stresses after annealing; in what follows, attention will rather be given to the non-constant $E$ part of the residual stress field, which is here also referred to as the near-field region. The polyfit curves of Fig. 4 enable the kinetics of stress relaxation to be studied graphically for each location in the defined stress region. This has been done for a few selected locations in the near-field region at the two temperatures as shown in Fig. 8.

In Fig. 8 (as well as Fig. 9), the lines joining the data points serve only to aid in perceiving general trends in stress relaxation at the selected locations in the stress field.

Relative stress relaxation is compared in Fig. 8 at equivalent distances during annealing of the Vickers residual stress field at 540 and 630 °C. The shapes of the curves are

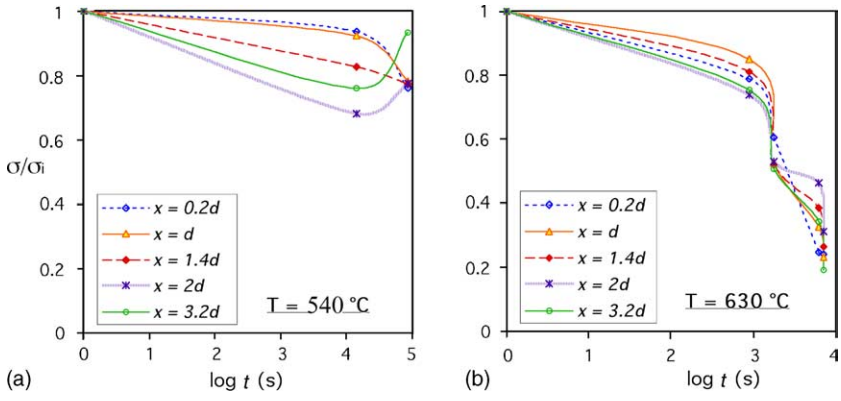


Fig. 9. Relaxation–log (time) plots on the near-field around the Vickers indent are different during isothermal holds at: (a) 540 °C and (b) 630 °C. The differing stress relaxation profiles suggest that different mechanisms predominate at the two temperatures. The curves joining the data points serve only to aid in perceiving general trends in relaxation at the two temperatures.

different for the two temperatures except at the edge where fast decreasing stresses give similar relaxation profiles with time.

At 540 °C, stress resurgence occurs at $\sim x > 1.5d$ after 4 h hold. Salomonson and Rowcliffe[4] found that compressive stresses changed sign and became tensile after long hold times at 550 °C. Scherer[28] also gives an account of a similar observation in a glass seal where the stress increased during isothermal hold for 4 h at 460 °C. The stress resurgence in the present study may be due to the tractions exerted on the surrounding matrix by the expansion of the transformed material against the plastic shell. After long hold times, the volume of transformed material has increased enough for the tractions to have a significant effect on the relaxation process. By contrast no increase in stress was observed anywhere with $T = 630$ °C. Here the reverse transformation of the entire plastic zone occurs quickly, implying that the plastic shell disappears within a relatively short time and is no longer there to influence the relaxation process as at 540 °C. It is likely that the different points in the residual stress region interact with one another.[28] Under such circumstances a stress relaxation profile that repeats itself from one point to another is not to be expected. Rather, the complex stress interactions lead to different transient stress profiles as depicted in Fig. 9, which are $\sigma/\sigma_i$–log time plots for the two experimental temperatures. $\sigma$ is the stress at the end of the hold time while $\sigma_i$ is the stress measured at the end of the heating stage, before isothermal hold begins. Examination of Fig. 9(a and b) shows that the relaxation profile changes from one sub-region of the near-field to another, and differs for each temperature. This implies that it is not possible to describe the stress relaxation of the Vickers residual stress field with a single master curve (see for example, Kurkjian,[29] Narayanawasmy,[30] Larsen et al.,[31] and van den Brink[32]) either for a particular temperature or for a range of temperatures. Stress relaxation must be described for each point in the stress field or at best for each well-defined sub-region.

On the basis of the foregoing it can be said that the Vickers residual stress field does not fulfil thermorheological simplicity as a region of material. Comparing the shapes of the curves for the same location at the two temperatures seems to confirm this, and the observation by Rekhson,[33] that glasses may exhibit non-linear behaviour due to the effect of mechanical stresses on structure. In reviewing the subject of mechanical relaxation in inorganic glasses Mazurin[34] notes that glasses show non-Newtonian flow when subjected to very high stresses.

## 4. Conclusions

The elastic response following the Oliver–Pharr method of analysing nanoindentation data has made it possible to study stress relaxation in the Vickers residual stress field. The size of material region studied is diminishingly small compared with sample sizes used in conventional stress relaxation experiments in glass (a conventional 1 cm × 1 cm sample size gives an area ratio of ~1600:1 with the Vickers residual stress field studied here). By using the Vickers indentation a region of material is created that is interesting in at least two aspects. First, a continuously changing residual stress field is created and second, the stresses thus generated are very high. Such regions are important since they offer the conditions for the study of glass behaviour outside the limitation of small strain and stress[35] and thus afford the opportunity to study glass in the light of non-linear viscosity. This work has thus shown that the Vickers residual stress field is not a thermorheologically simple region of material. Thus, a glass in its ordinary state may be thermorheologically simple but a mechanically excited region of it, such as that created by an elastic–plastic contact event, may not be necessarily so. Complete stress relaxation may not be achieved around an elastic–plastic indent in glass at 540 °C (or at $T < T_g$) unless sufficiently long hold times ($\gg$24 h) are employed. It may be that the stress relaxation of a mechanically induced stress state is tied with structural relaxation such that complete stress relaxation will not occur until structural equilibrium has been achieved. In situations involving high strains and structural distortions, as around a Vickers macroindent, the kinetics for structural relaxation at sub-$T_g$ temperatures may not favour complete return to structural equilibrium and the achievement of stress relaxation as a consequence. At 630 °C, the mechanical and chemical relaxation mechanisms have increased kinetics and a large amount of stress relaxation is achieved within a relatively short time. Stress relaxation is not uniform across the Vickers residual stress field but is fastest at the edge of the plastic impression. A substantial amount of the relaxation occurs already during the heating process before isothermal hold begins. One may infer from the definitions that "stress release occurs within a matter of minutes at the annealing point" and "within a matter of hours at the strain point"[36] and the results of the present study that, one effect of large mechanical excitations in glass is to shift the glass transition region to higher temperatures.

## Acknowledgement

The authors would like to thank Dr. Olena Smuk for the DSC measurements of the $T_g$ of the glass used in the study and Prof. Kjell Pettersson for reading and commenting parts of the manuscript.

## References

1. Marshall, D. B. and Lawn, B. R., Flaw characteristics in dynamic fatigue: the influence of residual contact stresses. *J. Am. Ceram. Soc.*, 1980, **63**, 532–536.
2. Chantikul, P., Lawn, B. R. and Marshall, D. B., Micromechanics of flaw growth in static fatigue: influence of residual contact stresses. *J. Am. Ceram. Soc.*, 1981, **64**, 322–325.

3. Pajares, A., Guiberteau, F., Steinbrech, R. W. and Dominguez-Rodriguez, A., Residual stresses around Vickers indents. *Acta Metal. Mater.*, 1995, **43**, 3649–3659.
4. Salomonson, J. and Rowcliffe, D., Removal of residual stress at controlled surface flaws. In *Indentation Fracture of Alumina and Glass*. Appendix II in Ph.D. thesis, Royal Institute of Technology, Stockholm, Sweden, 1996.
5. Roach, D. H. and Cooper, A. R., Effect of contact residual stress relaxation on fracture strength of indented soda-lime glass. *J. Am. Ceram. Soc.*, 1986, **68**, 632–636.
6. Kese, K. O., Li, Z. C. and Bergman, B., Influence of residual stress on elastic modulus and hardness of soda-lime glass measured by nanoindentation. *J. Mater. Res.*, 2004, **19**, 3109–3119.
7. Arora, A., Marshall, D. B., Lawn, B. R. and Swain, M. V., Indentation deformation/fracture of normal and anomalous glasses. *J. Non-Cryst. Solids*, 1979, **31**, 415–428.
8. Han, W. T., Hrma, P. and Cooper, A. R., Residual stress decay of indentation cracks. *Phys. Chem. Glasses*, 1989, **30**, 30–33.
9. Oliver, W. C. and Pharr, G. M., An improved technique for determining hardness and elastic modulus using load and displacement sensing indentation experiments. *J. Mater. Res.*, 1992, **7**, 1564–1583.
10. Mallinder, F. P. and Proctor, B. A., Elastic constants of fused silica as a function of large tensile strain. *Phys. Chem. Glasses*, 1964, **5**, 91–103.
11. Ernsberger, F. M., In *Glass: Science and Technology* (*Vol 5*), ed. D. R. Uhlmann and N. J. Kreidl. Academic Press, New York, 1980, pp. 10–11.
12. Jarausch, K. F., Keily, J. D., Houston, J. E. and Russell, P. E., Nanoindentation as a probe of stress state. In *Proceedings of the Society of Experimental Mechanics Annual Conference on Theoretical, Experimental and Computational Mechanics (USA)*. g:1999:3, 1999, pp. 328–330.
13. Dahmani, F., Lambropoulos, J. C., Schmid, A. W., Burns, S. J. and Pratt, C., Nanoindentation technique for measuring residual stress field around a laser-induced crack in fused silica. *J. Mater. Sci.*, 1998, **33**, 4677–4685.
14. LaFontaine, W. R., Paszkiet, C. A., Korhonen, M. A. and Li, C.-Y., Residual stress measurements of thin aluminium metallizations by continuous indentation and X-ray measurement techniques. *J. Mater. Res.*, 1996, **6**, 2084–2090.
15. Fisher-Cripps, A. C., *Nanoindentation*. Springer-Verlag, New York, 2002, pp. 79–80.
16. Underwood, J. H., Residual-stress measurement using surface displacements around an indentation. *Exp. Mech.*, 1973, **30**, 373–380.
17. Zeng, K. and Rowcliffe, D., Experimental measurement of residual stress field around a sharp indentation. *J. Am. Ceram. Soc.*, 1994, **77**, 524.
18. Abe, H., Ikeda, K., Nakashima, H., Yoshida, F. and Koga, K., Evaluation of indentation induced residual stress in the surface of float glass. *J. Ceram. Soc. Jpn.*, 2000, **108**, 416–419.
19. Kese, K. and Rowcliffe, D. J., Nanoindentation method for measuring residual stress in brittle materials. *J. Am. Ceram. Soc.*, 2003, **86**, 811–816.
20. Chiang, S. S., Marshall, D. B. and Evans, A. G., The response of solids to elastic/plastic indentation. I. Stresses and residual stresses. *J. Appl. Phys.*, 1982, **53**, 298–311.
21. Shen, J., Green, D. J., Tressler, R. E. and Shelleman, D. L., Stress relaxation of a soda lime silicate glass below the glass transition temperature. *J. Non-Cryst. Solids*, 2003, **324**, 277–288.
22. James, M. R., Relaxation of residual stresses during fatigue. In *Sagamore Army Materials Research Conference Proceedings* (*Vol 28*), ed. E. Kula and V. Weiss. Plenum Press, New York, 1982, pp. 297–314.
23. Ghosh, A., Vaidyanathan, S., Gulati, S. T., Haggy, H. E. and Geisinger, K. L., Stress relaxation in alkali strontium silicate panels during subsequent thermal processing. In *Advances in Processing of Glass*. *Proceedings of the 3rd International Conference*, New Orleans, 10–12 June 1992. Am. Ceram. Soc. *Ceram. Trans.*, 1992, **29**, 354–364.
24. Scholze, H., *Glass: Nature, Structure and Properties*. Springer-Verlag, New York, 1990, p. 289.
25. Kese, K. and Tehler, M., Unpublished work.
26. Hagan, J. T., Shear deformation under pyramidal indentation in soda-lime glass. *J. Mater. Sci.*, 1980, **15**, 1417–1424.
27. Bartenev, G. M. and Scheglova, N. N., High-temperature relaxation mechanisms in inorganic glasses. *J. Non-Cryst. Solids*, 1980, **37**, 285–298.
28. Scherer, G. W., *Relaxation in Glass and Composites*. John Wiley and Sons, Toronto, 1986, pp. 186–188.
29. Kurkjian, C. R., Relaxation of torsional stress in the glass tranformation range of soda-lime-silica glass. *Phys. Chem. Glasses*, 1963, **4**, 128–136.
30. Narayanaswamy, O. S., Annealing of glass. In *Glass Science and Technology* (*Vol 5*), ed. D. R. Uhlmann and N. J. Kreidl. Academic Press, New York, 1986, pp. 275–318.
31. Larsen, D. C., Mills, J. J. and Sievert, J. L., Stress relaxation behaviour of soda lime glass between the transformation and softening temperatures. *J. Non-Cryst. Solids*, 1974, **14**, 269–279.
32. van den Brink, J. P., Master stress relaxation function of silica glasses. *J. Non-Cryst. Solids*, 1996, **196**, 210–215.
33. Rekhson, S. M., Viscosity and stress relaxation in commercial glasses in the glass transition region. *J. Non-Cryst. Solids*, 1980, **38/39**, 457–462.
34. Mazurin, O. V., Mechanical relaxation in inorganic glasses. In *Glass Science and Technology* (*Vol 5*), ed. D. R. Uhlmann and N. J. Kreidl. Academic Press, New York, 1986, pp. 119–179.
35. Rekhson, S. M., Viscoelasticity of glass. In *Glass Science and Technology* (*Vol 5*), ed. D. R. Uhlmann and N. J. Kreidl. Academic Press, New York, 1986, pp. 1–117.
36. Varshneya, A. K., *Fundamentals of Inorganic Glasses*. Academic Press, 1994, p. 190.